# 8.2 RETRIEVAL OF CLOUD PHASE OVER THE ARCTIC USING MODIS 6.7-12 μm DATA

Douglas A. Spangenberg*
Analytical Services & Materials, Inc., Hampton, Virginia

Patrick Minnis
NASA-Langley Research Center, Hampton, Virginia

Matthew D. Shupe
NOAA-ETL, Boulder, Colorado

Mike R. Poellot
University of North Dakota, Grand Forks, North Dakota

## 1. INTRODUCTION

With the establishment of the well-instrumented North Slope of Alaska (NSA) site by the Atmospheric Radiation Measurement (ARM) Program, the development of new techniques for interpreting cloud radar data, and dedicated field programs such as the Mixed-Phase Arctic Cloud Experiment (MPACE; Verlinde et al. 2005), it is possible to validate existing satellite retrieval methods and develop and test new polar cloud retrieval techniques, especially those for detecting mixed phase clouds. In this paper, a new multi-spectral mixed phase detection technique (MMDT) for classifying clouds as mixed, liquid, or ice phase is fashioned using a combination of radiances measured by the Moderate Resolution Imaging Spectroradiometer (MODIS) at 6.7, 7.3, 8.5, 11.0, and 12.0 μm together with the NSA and MPACE observations. The key part of the phase detection technique is an observationally derived water vapor and temperature parameterization of cloud phase. The parameterization works under the premise that each type of cloud system (and phase) has a unique atmospheric water vapor (WV) and thermal structure associated with it.

The MMDT is applied to an independent MODIS dataset and verified against other NSA and MPACE data. It is shown that the MMDT can achieve a high degree of accuracy in phase discrimination relative to the surface-based retrievals. In addition to its ability to detect mixed-phase clouds, the MMDT could be used to help identify thin cirrus clouds overlying mixed or liquid phase clouds (multiphase ice). Moreover, since it only uses the infrared (IR) part of the spectrum, the new method is robust in the sense that it can be applied to daytime, twilight, and nighttime scenes with no discontinuities in the output phase. The technique is an initial step in confronting the mixed phase problem in polar regions and should be applicable to any other satellite imager dataset having the requisite channels.

* *Corresponding author address:* Douglas A. Spangenberg, AS&M, Inc., Hampton, VA, 23666; e-mail: d.a.spangenberg@larc.nasa.gov

## 2. DATA

Satellite data used in this study consist of *Terra* and *Aqua* MODIS 1-km resolution 6.7 (T67), 7.3 (T73), 8.5 (T85), 11 (T11), and 12-μm (T12) radiances. The MMDT was developed using 100 selected overpasses that imaged a wide variety of cloud types from 2000-04. All overpasses encompassing Barrow from March-April 2000, July 2000, January 2003, August 2003, and 27 September-27 October 2004 were employed for the MMDT validation. To facilitate the comparison with the surface data, the MODIS pixel radiances were averaged onto a 10-km radius circular region centered at the ARM-NSA Barrow site. The radiance data were then converted into brightness temperatures using the Planck function; these brightness temperature (BT) data were used to develop and validate the MMDT.

Surface-based data used in this study were taken from the millimeter-wave cloud radar (MMCR), microwave radiometer (MWR), and radiosondes. The data sampling periods were chosen to match those of the satellite data mentioned above. These instruments are all based at the ARM-NSA site in Barrow. Additionally, data from National Weather Service radiosondes, launched from the Barrow airport, were used for times when the ARM data were either missing or incomplete. The surface multi-sensor (SMS) phase data are based on the MMCR 1-minute and 45 or 90-meter resolution time-height cross-sections and are described in

Shupe et al. (2005). The ice water path (IWP) was determined using an MMCR regression retrieval technique and liquid water path (LWP) was derived from the MWR (Shupe et al., 2001, 2005). Both LWP and IWP are required to estimate the ratio of liquid-to-ice water in mixed-phase clouds.

In-situ cloud data taken from the University of North Dakota Citation (CIT) aircraft, which flew during MPACE, were used to evaluate the MMDT. For this dataset, the liquid water content (LWC) was obtained from the King probe while total water content (TWC) was obtained from the cloud spectrometer and impactor (CSI) probe. For the CIT flights within 20 km of Barrow, LWC and TWC data were averaged in 10-minute intervals and then used to determine cloud phase. For the flight on 8 October 2004 along the northern coast of Alaska, the LWC and TWC data were binned into 2-minute average intervals in order to determine if the clouds were mixed along the flight path.

## 3. MULTI-SPECTRAL MIXED PHASE DETECTION TECHNIQUE (MMDT)

Five distinct clouds types were used to develop the MMDT. These include boundary layer liquid, low mixed, high mixed, high ice, and low ice. The clouds were partitioned according to the phase retrieved by the SMS method of Shupe et al. (2005). The 3-km level is used to separate the clouds into the low and high categories. The mean temperature (T) and dewpoint T (Td) profiles for the liquid, low mixed, and high ice-phase cases are shown in Fig. 1. Each cloud type has its own distinctive set of profiles. The liquid-phase clouds exhibit a lower, more pronounced T inversion with dry air above the shallow cloud tops compared to the low mixed-phase clouds. As expected, the liquid clouds also have a higher T for each tropospheric level. For cirrus clouds, the mean profile shows relatively dry air near the surface with a deep moist layer in the middle-upper troposphere.

The first part of the MMDT relies on the absorption coefficient $\kappa$ for ice and liquid water to obtain different radiance values depending on cloud phase. Given a negative T lapse rate and the fact that $\kappa$ for ice increases at a different rate than $\kappa$ for water between 8.5 and 12 $\mu$m, ice and liquid clouds should be distinct in BT difference (BTD) images in this wavelength interval. Ice clouds are expected to yield strongly positive values of the BTD between T85 and T11 (T85-11). Also of importance for mixed-phase cloud detection is the absorption characteristics of the MODIS 6.7-$\mu$m WV channel. Since the 6.7-$\mu$m $\kappa$ for ice is higher than the corresponding 8.5-$\mu$m value, this should lead to larger (positive) BTDs between T85 and T67 (T85-67) for clouds containing ice at their tops compared to ones that contain only liquid. For clouds below 3 km, there will be no effect from the absorption coefficient since the 6.7-$\mu$m radiance is limited to the middle-upper troposphere. The primary basis for the MMDT is that the BTDs between the MODIS WV channels should be different for each cloud phase. Since the MODIS WV channels detect radiation from different atmospheric layers depending on wavelength, the BTDs should mimic the particular T and WV profiles associated with each of the phase types. Due to the dry Arctic atmosphere, these BTDs will be primarily related to the T profile above the cloud top (Ztop). Because of the complex nature of polar cloud systems coupled with frequent T inversions, a series of BT and BTD threshold (THR) tests were developed to allow for more accurate phase classifications from the MMDT. The thresholds were developed by examining the MODIS BT data for those cases where the MMDT failed to retrieve the expected SMS phase. Essentially, these thresholds allow the cloud phase to be correctly categorized when anomalous T or WV conditions are present. Throughout this study, a mixed-phase cloud is considered to be one that has either stratified layers of liquid and ice or liquid and ice co-existing in the same volume of space. The liquid component of a mixed-phase cloud is supercooled.

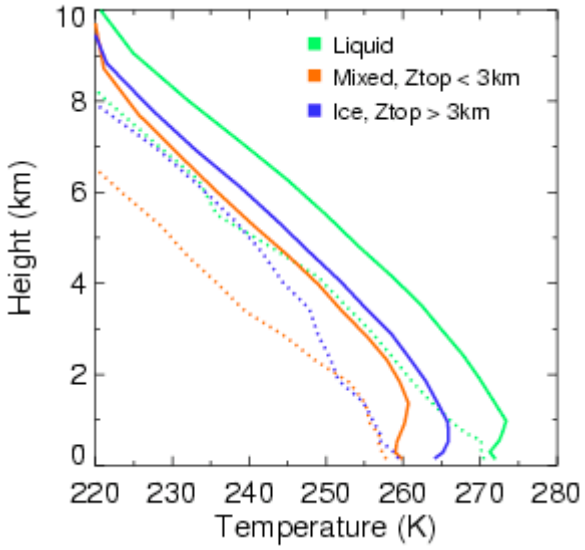


Figure 1. Mean sounding profiles for three of the cloud types used to develop the MMDT. Solid lines are for temperature and dotted lines are for dewpoint temperature. Ztop represents the cloud-top height.

### 3.1 *Infrared Trispectral Technique*

The starting point for the MMDT algorithm for polar clouds is the infrared trispectral technique (IRTST). The underlying premise behind this technique originally used by Strabala et al. (1994) is the difference between the absorption coefficients for water and ice. A set of imaginary indices of refraction $m_i$ for water and ice were obtained from Downing and Williams (1975) and Warren (1984), respectively. These indices are plotted in Fig. 2. The absorption coefficient will have a similar shape when compared to the imaginary index of refraction since the two are linked by the equation

$$\kappa = 4\pi m_i/\lambda. \quad (1)$$

Ice clouds absorb radiation much more effectively than water clouds at 11 μm with both cloud types being less efficient absorbers at 8.5 μm. Given a negative T lapse rate, ice clouds will exhibit a positive T85-11 since the radiation at 11 μm will be arriving at the satellite from a higher, colder level in the cloud. Contrary to the larger positive BTDs between T11 and T12 (T11-12) for water clouds found in the original non-polar IRTST, the opposite tends to be true for polar clouds because of the frequent T inversions and cold surface. For a water cloud with its top between the inversion base and peak, the higher $m_i$ in (1) for water at 12 μm compared to 11 μm (Fig. 2) will cause a negative T11-12 value since the radiation at 12 μm will arrive at the satellite from a higher and warmer level in the cloud. Yamanouchi et al. (1987) found that the T11-12 values in thin clouds tend to be higher when the cloud-top temperature is lower than the background surface and negative if the cloud top is warmer than the surface. This leads to differences in T11-12 between high cirrus clouds and boundary layer liquid or mixed-phase clouds trapped in the frequent temperature inversions.

Figure 3a shows the IRTST T85-11 and T11-12 scatter diagram for 100 cases from the years 2000-04 used to develop the MMDT. The different symbols indicate the surface-retrieved cloud phase. The selected cases represent a wide range of meteorological conditions so that many cloud types were sampled. Clouds with T85-11 values over 1.4 K are considered to have an ice phase. The other regions in Fig. 3a are those where mixed-phase clouds are typically found and consequently where the MODIS water vapor data

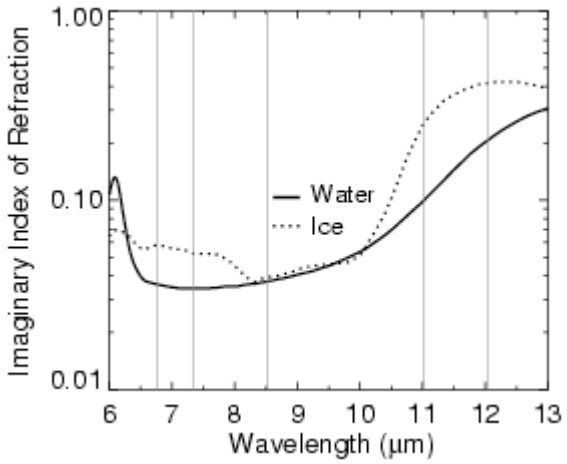


Figure 2. The imaginary index of refraction for water and ice in the 6-13 μm range. Vertical lines denote the wavelengths of the MODIS channels used in this study.

are required. Note, the greatest concentration of mixed-phase clouds are found roughly halfway between the ice and liquid cases. The exact location of a mixed-phase case on the IRTST plot (Fig. 3a) will not only depend on the amount of ice at cloud top, but also on the internal T profile in the upper portion of the cloud.

### 3.2 *Polar Cloud Phase Parameterization*

Although the differences in κ for water and ice between the MODIS WV channels (Fig. 2) will have a small influence on the BTD between them, the key part of the MMDT is a polar cloud phase parameterization (PCPP) based on T and WV profiles from Ztop to the tropopause. The PCPP works on the premise that a given cloud type will be associated with a unique pattern in the thermal and moisture profiles inside and above the cloud. Since the BTDs between the MODIS water vapor channels are coupled to the thermal and moisture structure of the atmosphere, they will be directly linked to the cloud type and hence cloud phase.

The amount of radiant energy detected by the satellite from each atmospheric level, also known as a contribution function (CF), was derived for each MODIS WV channel. To accomplish this, a correlated k-distribution technique originally applied to NOAA Advanced Very High Resolution Radiometer data by Kratz (1995) was adapted to compute the WV contribution functions for MODIS. Figure 4 shows the contribution functions associated with three different cloud types. The mean sounding conditions in Fig. 1 were used to obtain the CF profiles. Across the range of cloud

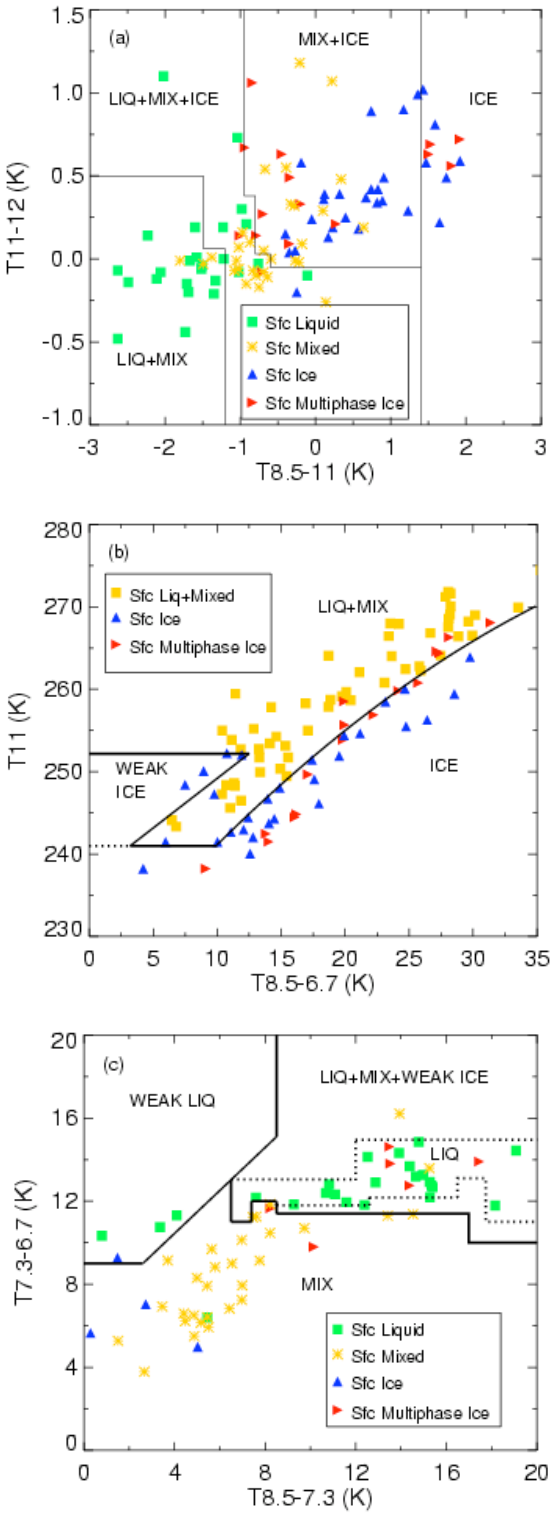


Figure 3. MMDT summary. Symbols denote surface-based phase type. (a) IRTST groups pixels into the initial phase categories, (b) shows IPP used to separate ice from mixed and liquid phases, (c) shows MPP used to distinguish mixed phase from liquid and multiphase ice. Dashed region shows conditions where liquid clouds are most likely to be found.

types, the 6.7-μm CF peaks between 5 and 7 km, the 7.3-μm CF peaks between 3 and 5 km, and the 8.5-μm CF peaks at the surface. The mean temperature profiles associated with low-level mixed clouds have the lowest CF peaks, with a significant part of the radiation at 7.3 μm arriving from the lower troposphere (Fig. 4b). Profiles associated with liquid clouds have the highest CF peaks (Fig. 4a) since they usually occur in relatively warm, moist environments. It should be noted that the cloud itself doesn't factor into the CF profiles; they are intended to show the atmospheric layer that is the source of most of the radiation detected by the satellite. Once a cloud is introduced, there will be a spike in the CF corresponding to Ztop with no contribution from below.

For the mixed phase and ice overlap region of Fig. 3a (top-center), and across the part of the diagram where all three phases are found, MODIS 6.7, 8.5, and 11 μm BT data are used to separate ice clouds from those containing at least some liquid. This subset of the PCPP is denoted as the ice phase parameterization or IPP and is shown in Fig. 3b, which plots all of the 100 cases used to develop the MMDT. The triangles are for the surface-retrieved ice and multiphase ice while orange squares represent liquid and mixed phase. MODIS pixels below the solid black line will usually be assigned the ice phase, which is in agreement with the surface phase retrievals. Most ice-phase clouds lie towards the lower-right part of the Fig. 3b diagram with high values of T85-67. This occurs because there is often a relatively large amount of water vapor above high ice clouds so that the radiation sensed by MODIS at 6.7 μm is from a layer mostly above cloud top (Fig. 4c) with the T85 radiation coming from inside the cloud. The T and Td profiles for high ice clouds shown in Fig. 1 indicate that on average, the upper layers are nearly saturated to the tropopause. Moreover, examination of the relative humidity (RH) at Ztop and the mean RH from Ztop to 1 km above the top (not shown) revealed no significant drop in RH. Also, for those cirrus clouds whose tops are sensed by MODIS at 6.7 μm, the higher κ value at 6.7 μm compared to that at 8.5 μm (Fig. 2) will lead to somewhat higher T85-67 values. For the mixed and liquid region in Fig. 3b above the black solid line, dry air exists above the cloud tops and T85-67 is driven primarily by the difference in temperature between the middle troposphere and Ztop. The SMS ice clouds in and near the weak ice region in Fig. 3b are a special subset of thin, boundary-layer clouds that do not show up well

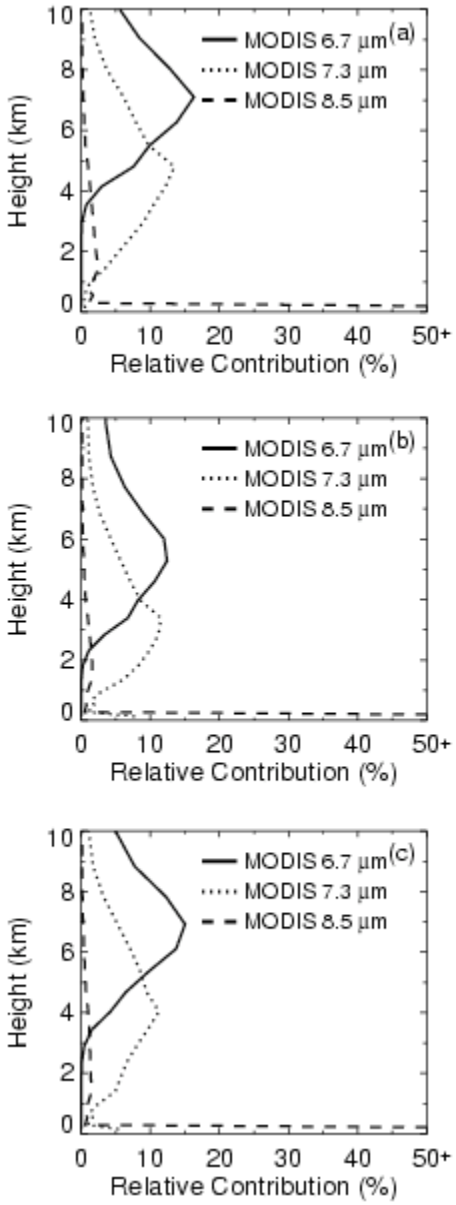


Figure 4. MODIS water-vapor channel contribution functions for mean sounding conditions associated with the main cloud types. (a) Liquid, (b) mixed, Ztop < 3km, and (c) ice, Ztop > 3 km.

in the MODIS imagery and some of these cases are likely to be diamond dust. If detected by MODIS, many of these clouds will be correctly classified as having an ice phase. Many of the multiphase ice cases, where thin cirrus overlies a mixed or liquid cloud, will be put into the ice phase. For those multiphase ice cases falling in the liquid and mixed region of the IPP, up to 33% of the individual imager pixels within 10 km of Barrow were grouped into the ice phase. This is the case because thin cirrus tends to be organized into streamers and filaments.

To assign a cloud phase to MODIS pixels in the liquid and mixed overlap region of the IRTST (Fig. 3a, lower-left), and for the part of the diagram where all three phases are found, only the MODIS WV BTD data are used. Since this subset of the PCPP is largely used to separate the mixed phase from the liquid phase, it will be referred to as the mixed-phase parameterization, or MPP. This part of the PCPP is depicted in Fig. 3c; it includes each of the mixed and liquid cases above the black solid line in Fig. 3b. Although the $\kappa$ for water and ice has some effect on the BTD between the MODIS 8.5 and 7.3 $\mu$m channels (T85-73), it does not aid the separation of the liquid from the mixed phase. This is because the separation is achieved primarily by the BTD between the MODIS 6.7 and 7.3 $\mu$m channels (T73-67). With mixed-phase clouds occurring in a wide variety of T, WV conditions in the Arctic, a larger part of the Fig. 3c diagram is devoted to them. The mixed-phase clouds in the upper-right-hand quadrant of Fig. 3c, where multiple cloud phases exist, are relatively warm with cloud-top temperatures generally above 260 K. These are the most difficult types of mixed-phase clouds to separate from the liquid phase. Warm-season liquid-phase clouds in the boundary layer only occur by themselves in a specific set of meteorological conditions and this is reflected by the tight cluster of liquid-phase cases in the upper-right part of Fig. 3c. The dashed-line region represents the location where warm-season liquid clouds are most likely to be found. The liquid-phase cases in the upper-left part of the diagram represent cold-season, or weak liquid, cases where large temperature inversions are found with the cloud trapped in the cold boundary-layer air. The four surface-retrieved ice-phase clouds on the left side of Fig. 3c are thin, low-level clouds that either cannot be seen in the MODIS imagery or show signs of having at least some liquid in them. In the upper-right part of Fig. 3c where weak ice clouds are found, T85-11, T11-12, T85-73, and T73-67 used together reveal that thin cirrus clouds can, at times, be separated from the relatively warm underlying scene.

### 3.3 *Threshold Tests*

To obtain agreement between the MMDT and SMS phase retrievals for a wider variety of T and WV conditions associated with polar clouds, a series of BT and BTD THR tests were established to complement the IRTST and PCPP. These tests, along with the other criteria used to determine cloud phase in the MMDT, are provided in Tables 1-3. The tests are arranged by the pixel's location

on the IRTST diagram (e.g., Fig. 3a). MODIS 11-μm BT data are used for the cloud T. Ice test 5 in Table 1 recognizes that a positive T85-11 and low value of T85-73 will occur primarily for cirrus clouds having negative internal T lapse rates across their tops. For these clouds, Ztop is well above the WV CF peaks at 8.5 and 7.3 μm. The main reason for adding ice THR tests 8 and 9 is to allow pixels the potential to become ice when they are originally grouped into the liquid and mixed region of the IRTST; given a positive internal T lapse rate, high ice clouds can appear as liquid or mixed clouds in the IRTST. However, applying the IPP with THR restrictions often reveals an ice cloud. These pixels will be grouped into the weak ice category. For the liquid clouds, Table 2 THR test 2 recognizes that mixed-phase clouds rarely, if ever, occur above a 270.5 K cloud T. Liquid phase THR tests 4 and 5 allow for mixed-phase clouds with relatively low temperatures to occur in the MPP liquid region (Fig. 3c).

The assignment of pixels to mixed phase occurs when they are in the mixed and ice region of the IRTST and mixed and liquid region of the IPP. For other areas of the IRTST, the MPP in Fig. 3c is consulted to assign the mixed phase. The mixed-phase pixels will have T11 values between 241 and 273 K. Tests 3 and 4 in Table 3 for mixed phase assume that mixed clouds occur under atmospheric T and WV conditions that are more variable than their standard liquid counterparts while test 6 turns an ice cloud into a mixed cloud given certain T, WV conditions when T11 is near the phase boundary of the IPP.

The order of the tests in the MMDT is critical to the outcome. First, any pixel with T11 > 273 K is assigned the liquid phase. Pixels having T11 < 241 K are then classified as ice clouds. For the remaining pixels, any one of the three phases can occur. Therefore, the IRTST is applied so the pixels can be grouped into one of four phase regions (Fig. 3a) and then passed on to the PCPP if necessary. The T85-67 and T11 values for pixels in the mixed and ice phase region of the IRTST (Fig. 3a, top center) are then checked and grouped into the ice or mixed phase according to the IPP (Fig. 3b; Tables 1, 3 Mix+Ice tests). For pixels falling into the IRTST liquid and mixed region, they are separated according to the MPP in Fig. 3c. Essentially, the pixels left behind after applying the liquid tests in Table 2 will be mixed. Also, if ice test 8 or 9 (Table 1) or mixed test 3 or 4 (Table 3) passes, the pixel will not be assigned the liquid phase when liquid tests 1-3 (Table 2) are invalid. For MODIS pixels in the liquid, mixed, and ice overlap area of the IRTST, the IPP (Fig. 3b) is consulted to check for ice pixels. If the pixel is not classified as ice, the MPP (Fig. 3c) is applied along with the appropriate THR tests to discriminate between the liquid and mixed phases. Finally, any pixel falling into the dashed liquid region of the MPP will have its T85-11 and T85-73 values checked to determine whether or not it has an ice signature.

## 4. RESULTS

To assess the performance of the MMDT, the SMS phase retrievals of Shupe et al. (2005) were compared to the MODIS-retrieved phase for 799 *Terra* and *Aqua* orbits representing four seasonal time periods during the years 2000-04. For the validation procedure, the MMDT output represents the dominant phase signal from 1-km pixel-level imager data averaged over a 10-km-radius circular region centered at Barrow. In order to be used in the validation dataset, the phase had to be constant in the SMS phase retrieval across the cloud top for, at least, 1 hour before and after the satellite overpass. Cloud top in this instance is defined as the upper-most 0.3 km of the cloud. The surface phase retrievals are considered to be the truth dataset.

The MMDT validation results are summarized in Table 4. The best agreement between MODIS and the surface phase retrievals are found during MPACE when uniform, boundary layer, mixed phase clouds are prevalent. The mixed phase agreement is at 91% for the 176 cases sampled while the ice phase agreement is at 94 % for the 88 cases sampled. In the deep Arctic night of January 2003, the MMDT correctly identified mixed-phase clouds with an 86% accuracy while the ice-cloud retrieval accuracy is at 92%. The months of July 2000 and August 2003 have the lowest matching percentages. This is a direct result of many transient, overlapping, multiphase cloud structures that existed then. Even taking this into account, the phase was correctly matched in at least 75 % of the cases. Moreover, an increase from 79 to 84 % in the matching ice cases can be seen if only considering those clouds over 1 km thick. For all four time-periods, the results were quite good, with matches of 90, 86, and 84 % for the liquid, mixed, and ice cases, respectively. For the 69 liquid cases sampled, 62 are supercooled indicating good discrimination between totally supercooled liquid water clouds and those containing at least some ice particles.

The primary factors that contributed to discrepancy between the MODIS and SMS phase retrievals include: thin ice clouds, the coastal

Table 1. MODIS ice-phase classification criteria. $T_{pb}$ is phase-boundary temperature. IRTST regions are defined in Fig.3a.

| IRTST region | Ice classification tests (T units in K) |
|---|---|
| All | (1) Cloud temperature: T <= 241 |
| Ice | (2) IRTST ice region (T85-11 > 1.4) |
| Mix+Ice | (3) IPP ice region<br>(4) IPP weak ice region, T85-11 > 0.10<br>(5) T85-11 > 0.55, T85-73 < 4.5; T85-11 > 0.35, T85-73 < 3.25<br>(6) IPP: Liq+Mix region, T < $T_{pb}$ + 4.0; MPP: Liq+Mix+Weak Ice region, T85-73 < 14.0; (T85-11 + T11-12) > 0.10 |
| Liq+Mix | (7) MPP: Liq region, T85-73 > 19.0, T73-67 < 12.0<br>(8) IPP: T85-67 > 23.5, T < $T_{pb}$-1.5; T73-67 < 14.5<br>(9) IPP: T85-67 > 25, T < $T_{pb}$; T11-12 > 0.15 |
| Liq+Mix+Ice | (10) Tests 3, 4, and 7 are applied<br>(11) MPP: Liq region; T85-11 > -0.50<br>(12) MPP: Liq region, T85-73 > 13; T85-11 > -1.0 |

Table 2. MODIS liquid-phase classification criteria.

| IRTST region | Liquid classification tests (T units in K) |
|---|---|
| All | (1) Cloud temperature: T > 273 |
| Liq+Mix, Liq+Mix+Ice | (2) T > 270.5<br>(3) T > 269, T85-11 < -2.2<br>(4) MPP: Liq region, T85-73 <= 8.5; T > 259.12<br>(5) MPP: Liq region, T85-73 > 8.5; T > 260.80<br>(6) MPP: Weak liquid region |

Table 3. MODIS mixed-phase classification criteria.

| IRTST region | Mixed-phase classification tests (T units in K) |
|---|---|
| All | (1) Cloud temperature range: 241 < T < 273 |
| Mix+Ice | (2) IPP Liq+Mix region; ice tests 5, 6 fail |
| Liq+Mix | (3) T85-67 < 27.9, T > 267.4, T85-73 > 12, T73-67 > 12<br>(4) T85-67 < 25, T > 266.5, T85-73 < 10.95<br>(5) MPP mix regions; ice and liq tests fail |
| Liq+Mix+Ice | (6) IPP: T85-67 > 26, T > $T_{pb}$-1.5; T73-67 > 14.96<br>(7) Tests 3-5 are repeated |

Table 4. MMDT and surface cloud phase matching for selected time-periods from 2000-04. Entries indicate percent of time MMDT agrees with surface retrievals. Number of samples indicated in parentheses. Ice-1 refers to ice clouds at least 1 km thick.

| | Matching % | | | |
|---|---|---|---|---|
| Time period | Liquid | Mixed | Ice | Ice-1 |
| Mar-Apr 2000 | ---- (0) | 83.7 (49) | 79.8 (114) | 86.6 (82) |
| Jul 2000, Aug 2003 | 89.3 (56) | 75.4 (69) | 78.6 (131) | 83.8 (80) |
| Jan 2003 | 83.3 (6) | 86.4 (44) | 91.5 (59) | 92.7 (41) |
| MPACE | 100.0 (7) | 90.9 (176) | 94.3 (88) | 94.7 (75) |
| All | 89.9 (69) | 86.1 (338) | 84.4 (392) | 88.8 (278) |

location of Barrow, uncertainties in the vertical partitioning of cloud phase in the SMS retrievals, and the time sampling of the surface data versus spatial averaging of satellite data. Several misclassifications occurred since Barrow is on the land but nearly 60% of the pixels within 10 km of Barrow are over the ocean. Land and ocean (with or without snow cover) can show different signatures for semi-transparent clouds since it is not uncommon for these background surfaces to be at different temperatures. Taking these factors into account, the MMDT validation results are remarkably good. For those times when the MMDT incorrectly retrieved liquid or ice instead of mixed phase, it reflected the dominant phase at the cloud top. Also, disagreement with the SMS retrievals were usually near a phase transition, indicating that a significant portion of the imager pixels will still be in agreement with the surface-retrieved cloud phase. Images where the MMDT misclassified the phase of the high, thin cirrus mainly occurred where the cloud was observed in the MMCR but was not very noticeable on inspection of the MODIS T11 imagery.

Once the phase is determined, it is important to know the relative amounts of liquid and ice in the mixed-phase clouds. To determine relative proportions of ice and water in the mixed phase clouds during MPACE, the LWP from the MWR was compared to the IWP retrieval from the surface-based sensors at the ARM-NSA Barrow site. Relative liquid (RLIQ) amounts, expressed as percentages, are given as

$$RLIQ_{sfc} = [LWP/(LWP+IWP)]*100, \qquad (2)$$

where the subscript *sfc* refers to the surface-derived values. For mixed-phase clouds, the surface RLIQ values at the satellite overpass times during MPACE are plotted in Fig. 5. The different symbols indicate the MMDT phase type. The relative amounts of liquid compared to ice in the clouds given by (2) are almost exclusively between 10 and 90%. There is a large cluster of RLIQ values ranging from 60-80% during much of the time period with a secondary cluster of values near 40% from days 283-290. For those three cases where the MMDT incorrectly retrieved the liquid phase, the relative amounts of liquid in the cloud were high, with values from 58-92%. Conversely, for the seven cases where the MMDT retrieved ice instead of the mixed phase, the RLIQ amounts were low, with values mostly less than 50%. Also plotted in Fig. 5 are 10-minute average data samples from the CIT when it was within 20

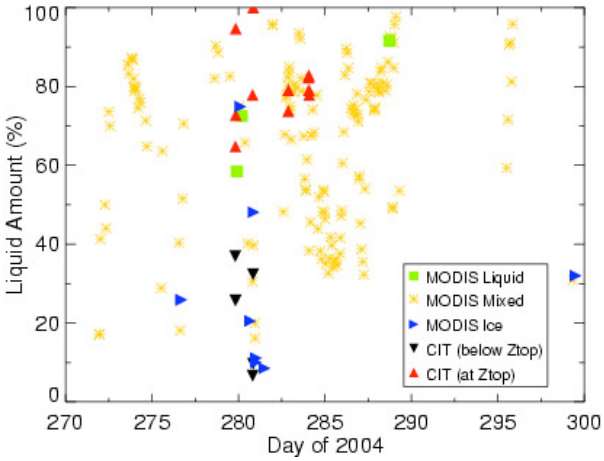


Figure 5. Surface-derived RLIQ in mixed-phase clouds for *Terra* and *Aqua* overpass times during MPACE as a function of MODIS phase type. Also shown are CIT RLIQ amounts for times when the aircraft was within 20 km of the ARM-NSA Barrow site.

km of Barrow. The downward-pointing triangles are for those times when the plane was at least 0.5 km or more below cloud top and the upward-pointing triangles represent times when it was within 0.5 km of cloud top. The RLIQ amounts for the CIT data were obtained using

$$RLIQ_{cit} = (LWC/TWC)*100, \qquad (3)$$

where the subscript *cit* refers to the in-situ-derived values. There is far more liquid in the clouds near the top compared to the amount deep inside the cloud, confirming the theory on low-level mixed-phase clouds. Moreover, there is good agreement between the CIT in-situ data, the MMDT retrievals, and the SMS retrievals.

For mixed–phase clouds, the T85-11 values found during MPACE were compared to T85-11 values in the multi-year dataset used to develop the MMDT. It is interesting to note that the BTD values are significantly lower during MPACE with a mean near –1.6 K whereas the multi-year dataset has a mean value closer to –0.8 K. This suggests that most of the mixed-phase clouds sampled during MPACE had large amount of liquid across their tops compared to the amount of ice. This is the boundary-layer stratus type of mixed-phase cloud with IRTST signatures matching those of pure liquid clouds. Close inspection of the Barrow soundings for each mixed-phase case used to develop the MMDT showed that the upper-most part of these clouds have positive T lapse rates since they extend a few hundred meters above the inversion base. The strong static stability and lack of strong, synoptic-scale vertical

motion will act to prevent the heavier ice crystals from being lifted all the way to the cloud top.

To show the spatial extent of the MMDT results, the Clouds and the Earth's Radiant Energy System (CERES) cloud mask developed by Trepte et al. (2002) was first applied to the *Terra* MODIS imagery taken at 2210 UTC 8 October 2004. This is a case when the CIT was flying along Alaska's northern coast between Deadhorse and Barrow during MPACE. The T67 image was then filtered using a 2-dimensional fast-Fourier transform technique to remove noise from the image's power spectra. The resulting cloud phase image from the MMDT and the corresponding satellite imagery are shown in Fig. 6. The T11 image (Fig. 6a) shows a stratus cloud with BT values ranging from 255-265 K. The thickest part of the cloud is south of Barrow where T85-73 (Fig. 6c) is lowest. The T85-11 image (Fig. 6b) shows that a relatively large amount of liquid exists on top of the stratus with T85-11 values near –1.0 K. Also, T11-12 values are below 0.0 K (not shown) so the pixels will lie in the lower-left, or liquid and mixed, region of the IRTST diagram. Most of these cloud systems are mixed with the periphery showing some liquid phase in the areas where the cloud is warmer in the T11 imagery (compare Figs. 6a, d). The most prominent mixed-phase cloud system is over central Alaska where the T85-73 values are below 8 K (Fig. 6c). These clouds will lie in the lower-left part of the MPP diagram (Fig. 3c), away from most of the liquid points. The traditional cloud phase detection method using the T85-11 image in Fig. 6b would reveal mostly liquid clouds with scattered pockets of ice in the eastern sections of the domain. The only cloud system containing all ice lies over the far northeastern corner of the domain in a region where T11 is low and both T85-11 and T11-12 are large.

Comparing the MMDT phase image in Fig. 6d to the Barrow SMS retrieval shows that both report mixed-phase clouds. For the CIT flight, the phase was determined by averaging the LWC and TWC in 2-minute intervals with (3) being used to obtain the RLIQ amounts. Clouds with an RLIQ amount of 10-90% are considered to be mixed phase. Figure 6d shows the CIT flight path, plotted in gray shades to indicate the cloud phase. Liquid and some mixed phase regions of the cloud dominate the segment with the largest stretch of unbroken liquid occurring when the aircraft was flying parallel to the coast and in the top of the stratus deck. Data from the CIT track indicate the cloud is mixed and dominated by the liquid component. This is in agreement with the MMDT and SMS phase retrievals.

## 5. SUMMARY

In this study, a MODIS cloud-phase classification technique was developed for polar cloud systems, with the primary aim of discriminating mixed-phase clouds from those containing a single phase. It can be used to gain a better understanding of mixed-phase clouds by providing information on their spatial extent and temporal variability. The algorithm starts with an IR trispectral technique utilizing the fact that the absorption coefficient for ice and liquid water will increase differently as wavelength increases from 8.5-12 μm. Since mixed-phase clouds can appear to be either all ice or all liquid water when using this technique, it was combined with a polar cloud-phase parameterization where the phase is assigned according to the MODIS water vapor and 11-μm BT data. In this way, the multi-spectral mixed-phase detection technique is able to clearly identify mixed, liquid, and ice phase clouds as separate entities. The technique has the capability to detect mixed phase clouds even when mostly liquid water or ice is found at their tops. A set of 271 cases examined during the Mixed-Phase Arctic Cloud Experiment revealed that the MODIS cloud-phase detection technique correctly identified 91% of the mixed-phase clouds. The ice phase was correctly identified 94% of the time. For the mixed-phase clouds sampled during MPACE, the LWP and IWP from the surface-based retrievals and the CIT in-situ data confirmed that they generally had between 10 and 90% liquid water relative to the amount of ice. Using the IRTST revealed that the most of the mixed-phase clouds that existed during MPACE had large amounts of water relative to ice at their tops.

Expanding the comparisons to a total of 6 months spanning all seasons over Barrow showed a MODIS phase classification accuracy of 84-90% when considering all phase types. For times when the MODIS phase classification technique didn't match the ground-based mixed-phase retrievals, it labeled the clouds with a phase that is consistent with the dominant phase found at cloud top. The MMDT also showed an ability to correctly identify the ice phase in the upper-most cloud deck for multilayered clouds. The main strength of the MODIS cloud-phase classification technique is that it will work just as well in cloud shadows, nighttime, and twilight scenes as it does for fully sunlit conditions. However, it is unclear how it will perform over highly elevated terrain such as the Antarctic plateau. Also, near phase transitions, the technique may have some difficulties due to abnormally moist or dry layers that can sometimes

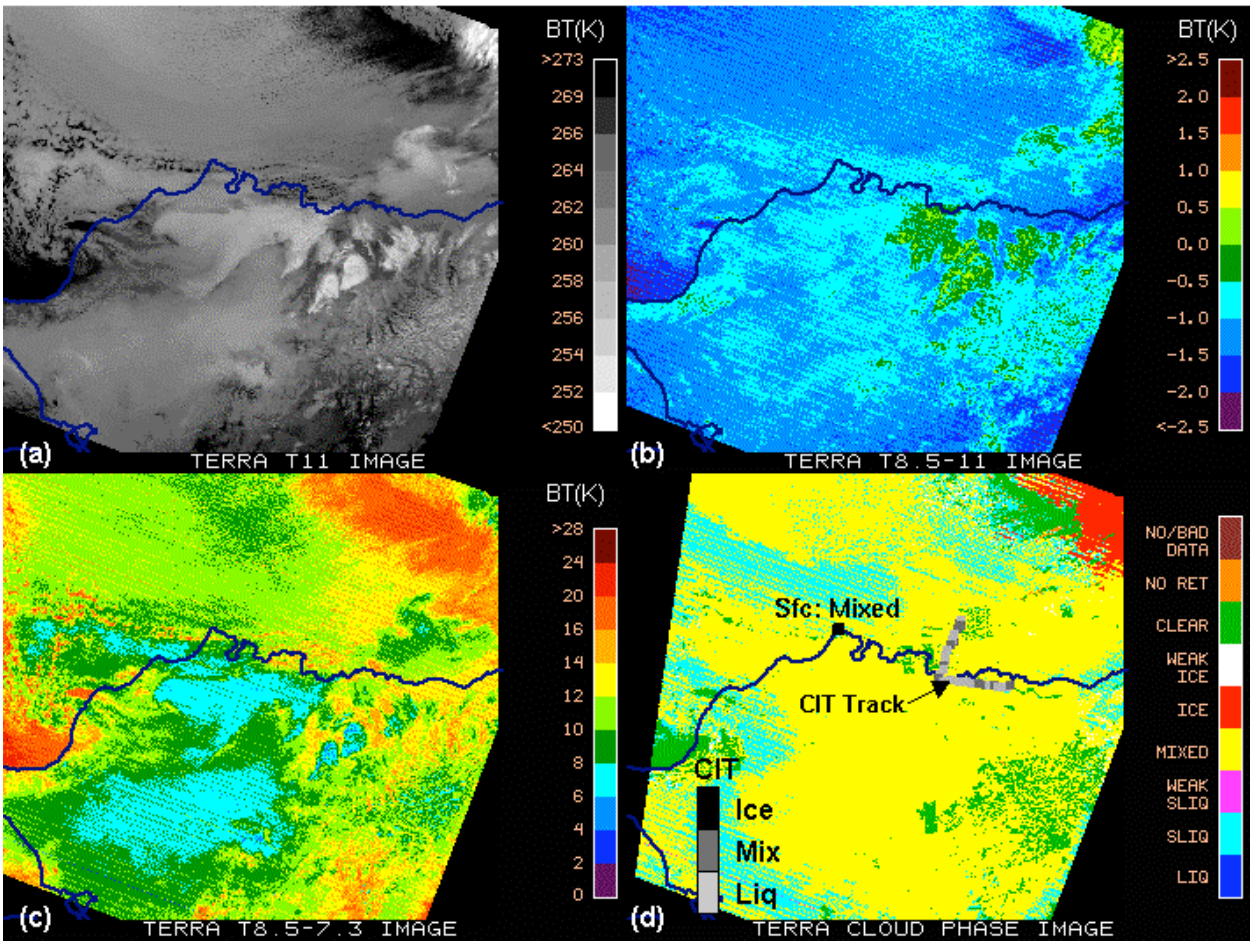


Figure 6. Terra-MODIS imagery for 2210 UTC 8 Oct 2004. (a) T11, (b) T85-11, (c) T85-73, and (d) cloud phase. Also plotted on (d) are the surface-based phase retrieval and the CIT flight track. Gray shades indicate the phase sampled by the CIT. The LIQ and SLIQ terms in the phase colorbar represent liquid and supercooled liquid, respectively.

exist above the cloud top. Finally, thin cirrus clouds over warm surfaces pose a problem since the clouds may have a mixed or liquid signature due to low T85-11 background values. In this type of scene, the underlying cloud phase will be retrieved if the cirrus is near the threshold limit of being detected by MODIS.

Once polar clouds and their phase have an accurate representation in the satellite data, the next step is to use the methods of Minnis et al. (2003) and Platnick et al. (2001) to determine the cloud microphysical properties. The current algorithms are set up to detect and process the ice and liquid phase only and presently cannot be tuned to retrieve polar cloud properties. Since low-level mixed-phase clouds tend to have liquid at their tops, a realistic droplet size can likely be retrieved from MODIS. However, since they can have pockets of larger ice crystals and drizzle at their tops, satellite effective liquid droplet sizes will sometimes be overestimated. For those mixed-phase clouds having an IRTST liquid signature, or that are trapped under the inversion, the PCPP can be consulted to find out how far the pixel lies from the pure liquid signatures. Using this information, along with other parameters such as cloud-top temperature, it may be possible to adjust the effective droplet size downward if necessary. Also, the current satellite algorithms produce ice crystal diameters that are either too small or non-existent for low-level mixed-phase clouds because of the dominant liquid-water signal. It may be possible to develop a parameterization of the ice crystal diameter for these mixed-phase clouds in terms of cloud temperature, optical depth, water droplet size, and the atmospheric thermal and water vapor structure. Similar methods can be implemented to improve MODIS effective particle size retrievals in mixed-phase clouds where the ice phase dominates at cloud top.

To view NASA-Langley cloud products at ARM-NSA and other ARM sites, please see the web page, http://www-pm.larc.nasa.gov.

## 6. ACKNOWLEDGEMENTS

Special thanks are given to Dave Kratz for helping with the MODIS water vapor contribution functions and to Mandy Khaiyer for running the CERES-MODIS cloud mask. This research was supported by the Environmental Sciences Division of U.S. Department of Energy Interagency Agreement DE-AI02-97ER62341 under the ARM program and by the NASA Aviation Safety Program through the NASA Advanced Satellite Aviation-weather Products Initiative. Radiosonde data were obtained from the ARM Program sponsored by the U.S. Department of Energy, Office of Science, Office of Biological and Environmental Research, Environmental Sciences Division.

## 7. REFERENCES

Downing, H. D. and D. Williams, 1975: Optical constants of water in the infrared. *J. Geophys. Res.*, **80**, 1656-1661.

Kratz, D. P., 1995: The correlated k-distribution technique as applied to the AVHRR channels. J. Quant. Spectrosc. Radiat. Transfer, **53**, 501-517.

Minnis, P., D. F. Young, S. Sun-Mack, P. W. Heck, D. R. Doelling, and Q. Z. Trepte, 2003: CERES cloud property retrievals from imagers on TRMM, Terra, and Aqua. *Proceedings of the SPIE 10th Intl. Symp. Remote Sens., Conf. on Remote Sens. Clouds and Atmos.*, Barcelona, Spain, September 8-12, 37-48.

Platnick, S. J., Y. Li, M. D. King, H. Gerber, and P. V. Hobbs, 2001: A solar reflectance method for retrieving cloud optical thickness and droplet size over snow and ice surfaces. *J. Geophys. Res.*, **106**, #D14, 15,185-15,199.

Shupe, M. D., T. Uttal, S. Y. Matrosov, and A. S. Frisch, 2001: Cloud water contents and hydrometeor sizes during the FIRE Arctic Clouds Experiment. *J. Geophys. Res.*, **106**, D14 15,015-15,028.

Shupe, M. D., T. Uttal, and S. Y. Matrosov, 2005: Arctic cloud microphysical retrievals fromsurface-based remote sensors at SHEBA. *J. Appl. Meteor.* In press.

Strabala, K.I., S.A. Ackerman, and W.P. Menzel, 1994: Cloud properties inferred from 8-12-μm data. *J. Appl. Meteor.*, **33**, 212-229.

Trepte, Q. Z., P. Minnis, and R. F. Arduini, 2002: Daytime and nighttime polar cloud and snow identification using MODIS data. *Proceedings of the SPIE Conf. on Optical Remote Sens. of the Atmosphere and Clouds III*, Hangzhou, China, Oct. 23-27.

Verlinde, J., J. Y. Harrington, G. M. McFarquhar, J. H. Mather, D. Turner, B. Zak, M. R. Poellot, T. Tooman, A. J. Prenni, G. Kok, E. Eloranta, A. Fridlind, C. Bahrmann, K. Sassen, P. J. DeMott, and A. J. Heymsfield, 2005: Overview of the Mixed-Phase Arctic Cloud Experiment (M-PACE). *Proceedings of the AMS 8th Conf. on Polar Meteorology and Oceanography*, Am. Meteorol. Soc., Boston, MA.

Warren, S. G., 1984: Optical constants of ice from the ultraviolet to the microwave. *Appl. Opt.*, **23**, 1206-1224.

Yamanouchi, T., K. Suzuki, and S. Kawaguchi, 1987: Detection of clouds in Antarctica from infrared multispectal data of AVHRR. *Journal of the Meteorological Society of Japan*, **65**, #06, 949-961.